

# Magnetic Field in the Outer Heliosphere

Edward J. Smith

*Earth and Space Sciences Division, Jet Propulsion Laboratory, Pasadena, CA 91109, USA*

**Abstract.** Observed properties of the magnetic field in the outer heliosphere are generally well described by the Parker model but evidence has accumulated of significant departures in the components and field magnitude. The radial component is independent of solar latitude at both solar minimum and maximum implying non-radial solar wind flow near the Sun driven by differential magnetic pressure. The azimuthal component deviates from the Parker values at high latitudes as a result of the non-radial flow near the Sun that causes fields to originate at higher latitudes than those at which they are observed far from the Sun. A turning of the spiral angle toward the radial direction by tens of degrees is often observed inside co-rotating rarefaction regions (dwell). A recent model attributes this effect to a motion of the field across polar coronal hole boundaries that results in different solar wind speeds along parts of the field line. The north-south component can depart from zero for many days as a result of the tilting of the interface between fast and slow streams. Recent Voyager observations show that, during solar minimum, the field magnitude is smaller than extrapolations outward from 1 AU. This “flux deficit,” seen earlier in Pioneer data, may be explained by any of several physical models.

## INTRODUCTION

The following is a review of the heliospheric magnetic field (HMF) beyond the orbit of Earth. The observed properties to be discussed are the three field components, BR, BT and BN, and the magnitude, B. Recent Ulysses results are emphasized since they are providing a greatly improved view of the three dimensional heliosphere. The solar source of the field and large-scale solar wind structures are discussed where relevant. The Parker model [1] provides the standard against which the observations are compared. Where significant departures are observed, more recent models are invoked that can explain the differences.

## OBSERVATIONS

The three components are presented in the usual Solar Heliographic (SH) coordinates (introduced many years ago by Leverett Davis, Jr.) also known as RTN coordinates. The **R** component is directed radially outward from the Sun to the spacecraft. The other prime vector is the Sun’s rotation axis (**H**) that, with **R**, defines the **T** axis (**H**×**R**), parallel to the solar equator and positive in the direction of solar rotation. The **N** component completes the orthogonal set (**N** = **R**×**T**). These axes correspond to the usual spherical polar coordinates (**R** = **e<sub>r</sub>**, **N** = −**e<sub>θ</sub>** and **T** = **e<sub>φ</sub>**) and facilitate comparison with Parker’s model.

CP719, *Physics of the Outer Heliosphere: Third International IGPP Conference*,  
edited by V. Florinski, N. V. Pogorelov, and G. P. Zank

© 2004 American Institute of Physics 0-7354-0199-3/04/\$22.00

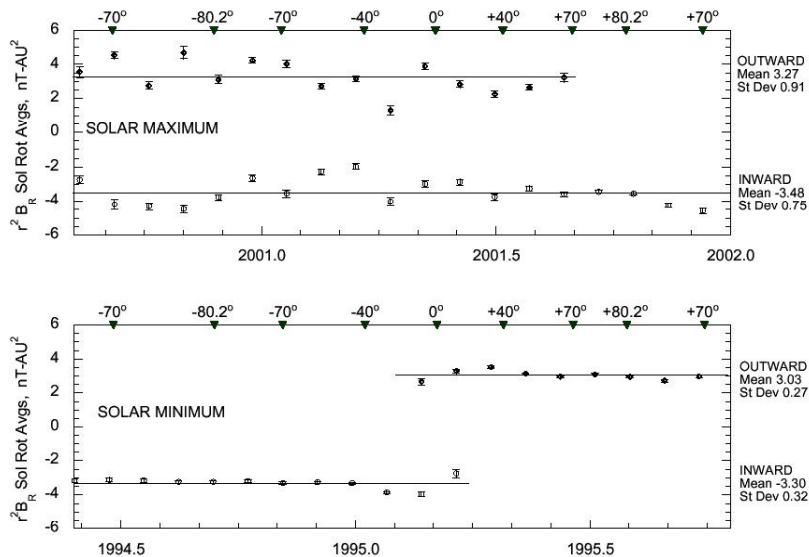


**FIGURE 1.** Ulysses measurements of the radial field component multiplied by the square of the distance to the Sun are shown between  $\pm 70^\circ$  heliographic latitude at both solar minimum and maximum. The open circles are solar rotation averages and the associated bars are the standard deviations. The straight lines are least squares fits to the averages (for the two magnetic sectors) and their mean values and standard deviations appear at the extreme right. (From [2]).

## Radial Component

Recent Ulysses measurements of  $B_R$  appear in Fig. 1, a plot of  $r^2 B_R$  during both solar minimum (lower panel) and maximum (upper panel), where  $r$  is radial distance [2]. Solar rotation averages are plotted as a function of time for the two South-to-North fast latitude scans in 1994–1995 and 2000–2001. Heliographic latitude appears along the two upper scales with the equator crossings located in the middle of the figure. The important feature is the absence of a dependence of the radial component on latitude at both solar minimum and maximum. This unexpected result implies non-radial solar wind flow near the Sun driven by differential magnetic pressure at the coronal source that results in the magnetic flux becoming uniformly distributed within a few solar radii [3]. Beyond this equilibrium distance, the solar wind flow is radial (except for fast-slow stream interactions that cause departures of only a few degrees). The Parker model is based on radial flow and is still applicable beyond a few solar radii, but the non-radial flows close to the Sun have been incorporated into newer models of the magnetic field with important consequences.

The streamline invariant,  $r^2 B_R$ , is a measure of open magnetic flux. Since it is independent of latitude,  $B_R$  measurements, including those in the ecliptic plane, are a

measure of the total open flux from the Sun [2]. In-ecliptic measurements of  $B_R$  for the past four sunspot cycles indicate that the open flux varies only slightly (by much less than a factor of two) between successive minimum and maximum in contrast to closed photospheric magnetic flux which varies by at least an order of magnitude. Fisk and Schwadron [4] have proposed that the open flux tends to be invariant because reconnection between open and closed field lines results in another pair of open and closed fields. However, even modest variations in  $B_R$  and especially the larger variations in  $B$  may have important consequences for other heliospheric constituents such as galactic cosmic rays.

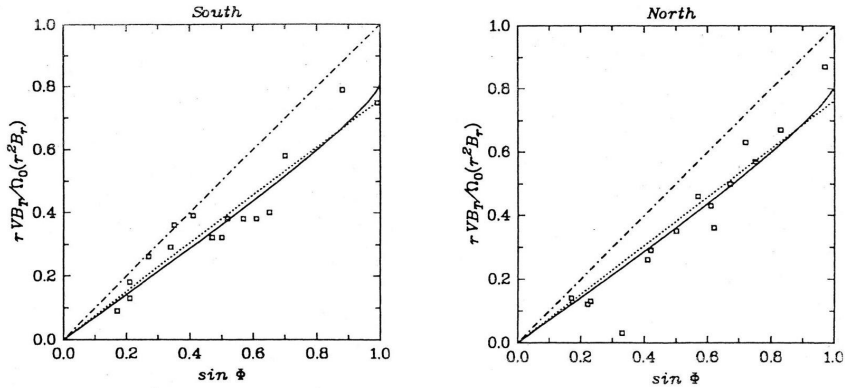


**FIGURE 2.** Ulysses measurements were used to derive the parameter shown based on Parker's model that is equivalent to the ratio of the solar rotation rate to the equatorial rate. The measured values are the squares that follow the least-squares straight line (dotted) but clearly deviate from the (dot-dash) straight line corresponding to  $\Omega = \Omega_0$ . Results are shown for both solar hemispheres as a function of the sine of the co-latitude ( $\phi$ ). The solid line is a fit to the observations based on the model of Banaszkiewicz, Axford and McKenzie. (From [6])

### Azimuthal Component and Spiral Angle

According to the Parker model,  $B_T$  is derived from  $B_R$  and depends on radial distance, solar wind speed,  $V$ , the angular rate of rotation of the Sun,  $\Omega$ , and the colatitude,  $\theta$ , i.e.,  $B_T = B_R (-\Omega r \sin \theta / V)$ . Measurements of  $B_T$ ,  $B_R$  and  $V$  at Ulysses have been used to study the rate at which the footprints of the field lines rotate at the Sun and, hence, to determine the heliographic latitude of origin. Figure 2 shows Ulysses measurements based on the above equation equivalent to  $\Omega / \Omega_0$ , where  $\Omega_0$  is the equatorial rotation rate, as a function of  $\sin \phi$  ( $\phi$  is colatitude in this instance) using the measured solar wind speed [5]. If the field line rotated rigidly at the equatorial rate, the points would lie along the straight (dot-dash) line. Ulysses measurements (squares) and the corresponding straight line fit (represented by the dotted line) deviate from  $\Omega = \Omega_0$  at essentially all latitudes. The deviations cannot be attributed alone to a dependence of  $\Omega$  on latitude.

Departures from the Parker model can be accounted for by a model that includes non-radial flow and non-radial field lines near the Sun (as well as a dependence of  $\Omega$  on latitude based on solar observations) [6]. Calculations of the equivalent  $\Omega / \Omega_0$  based on such a model are shown by the solid curve that passes through the observations. The non-radial fields and the independence of  $B_R$  on latitude close to the Sun cause the foot of the field lines to be located at higher latitudes than those inferred by taking the latitude of the spacecraft and simply extrapolating radially back to the Sun.

Not all significant departures from Parker's model can be accounted for in this way. Large departures of the observed spiral angle ( $B_T/B_R$ ) from the Parker spiral of up to  $30^\circ$ – $45^\circ$  are often observed inside Co-rotating Rarefaction Regions (CRRs) [7]. These solar wind structures are the complement of Co-rotating Interaction Regions (CIRs). At the coronal hole source, the steep gradient between slow and fast wind at the leading edge of the coronal hole boundary widens with distance as a result of compression of the slow wind and trailing fast wind. Correspondingly, the steep gradient at the trailing edge of the coronal hole where the speed falls from fast to slow also produces a widening solar wind region with distance, the CRR, in which the field magnitude and density drop to low values. The CRRs have also been known for many years as “dwells” because, when the gradually decreasing speed is propagated back to the Sun, the solar wind inside the CRR is found to originate (or dwell) at a common solar longitude or a narrow range of longitudes, usually the trailing edge of a coronal hole.

Figure 3 contains a plot of the field direction expressed in terms of the two angles,  $\theta$  and  $\phi$ . The coordinates are rotated so that  $\theta = 0$ ,  $\phi = 0$  coincides with the direction of the Parker spiral, based on the equation above with  $\tan(\phi) = B_T/B_R$ , and  $B_N = 0$  (because the Parker model assumes a radial solar wind velocity and a radial magnetic field at the Sun). (In this representation,  $\theta$  is the latitude, not the co-latitude, angle.) The data were obtained inside a CRR over many days as indicated. The contours of constant frequency of occurrence in the angle-angle plot show a large deviation on average from the Parker spiral (0,0). A histogram of  $\phi$  is included in the figure and shows the same large departure of the most probable value from the direction of the Parker field ( $\phi = 0$ ). No such departures are observed inside CIRs.

This deviation of the field inside CRRs that leads to fields that are more radial than predicted by the Parker model has been puzzling. A suitable explanation has recently been provided [7, 8]. It is an extension of the HMF model developed by Fisk [9]. The Fisk model includes several effects not present in the Parker model: a non-axisymmetric (tilted) polar coronal hole rotating rigidly at  $\Omega_0$ , differential rotation of the underlying photospheric magnetic field, non-radial solar wind flow near the Sun and continuous magnetic reconnection as the field rotates from inside to outside the coronal hole. The essential effect takes place at the trailing edge of the hole which forms the CRR at large distances. At the boundary, the solar wind speed drops from fast to slow so that, as the field line crosses the boundary, parts are propagated outward at different speeds. At large distances, the field line follows the Parker spiral corresponding to fast wind while nearer the Sun the shape of the field line is given by

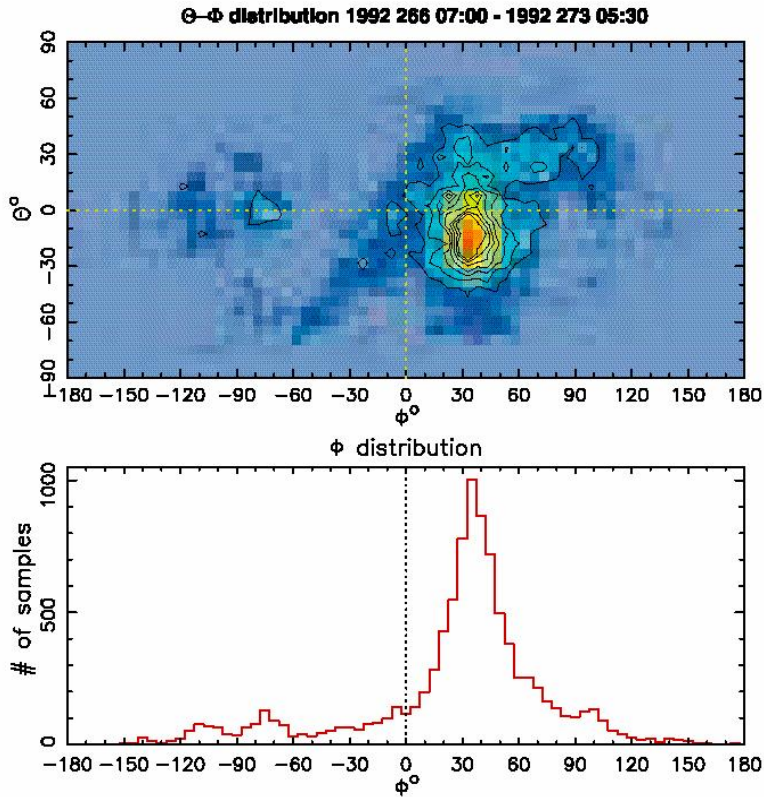


**FIGURE 3.** The field direction at Ulysses is represented by the latitude and azimuthal angles (above) and by the histogram of the spiral angle (below). The center of the upper (contour) plot is the direction along the Parker spiral as is  $\phi = 0$  in the histogram. The probability contours show a deflection of the field that is southward and westward (under-wound or more radial) over this seven-day interval while Ulysses was inside a rarefaction region. The most probable orientation of the field deviates from the Parker spiral by  $> 30^\circ$ . (From [7])

the Parker streamline for the slow wind. In between, the field turns toward the radial direction to connect the inner and outer spirals. Using reasonable parameters for the rate of rotation of the field, fast and slow solar wind speeds and the thickness of the boundary (the speed gradient), departures of  $30^\circ$  to  $45^\circ$  are readily obtained [7, 8].

### The North-South Component

As mentioned above, in the Parker model,  $B_N = 0$ . The long history of measuring the HMF shows that this component is indeed zero when averaged over intervals from days to solar rotations. However,  $B_N$  can depart significantly from zero for hours to

days (excluding the north-south fields often found inside Coronal Mass Ejections). An example of this behavior appears in Fig. 3 where a systematic variation in  $\theta$  along with  $\phi$  is seen, a variation shaped like an S lying on its side. Typically, large deviations in  $\theta$  appear in CIRs as well as CRRs.

The explanation for this behavior resides in the 3D aspects of the interaction between different speed solar wind streams. To a reasonable degree of approximation, contours of solar wind speed can be considered to follow the quasi-sinusoidal variation of the HCS in solar latitude and longitude. The HCS is surrounded by a band of slow speed wind with higher speed wind both above and below the slow wind. As the Sun rotates, fast wind overtakes slow wind that is trailing the HCS at specific locations causing the formation of a Stream-Stream Interface (SSI) and the surrounding CIR. Since the speed contours, the HCS and the SSI are generally tilted relative to the solar equator, deflections of the solar wind velocity and magnetic field vectors occur in north-south as well as east-west directions (a 3D variation of the “slow-east / fast-west” deflections of the solar wind in the equatorial/ecliptic plane). This tilting of the Interface leads to the propagation of the forward and reverse shocks away from and toward the solar equator (as observed by Ulysses). The magnetic field angle-angle plot is a method of identifying “planar magnetic structures” commonly found throughout most of a CIR with the same orientation as the Interface [10].

Approximately half a solar rotation later, fast wind precedes slow wind and the embedded HCS leading to the formation of a CRR as the fast and slow wind separate. Since the speed contours and HCS are also tilted in this region (as explained above, the wind and field typically issue from the edge of a polar coronal hole), the plane of symmetry is also tilted or inclined to the solar equator as in the case of the CIR. Thus, the characteristic “tilting” that takes place in these regions accounts for the prolonged intervals of north-south components of the field.

## Field Magnitude

Since the Parker model describes the three field components, it also predicts how the field magnitude will decrease with distance, namely,  $B = B_R [1 + (\Omega \sin\theta r/V)^2]^{1/2}$  and, since  $B_R$  is proportional to  $1/r^2$ ,  $B$  decreases like  $1/r$  at large distances.  $B$  also depends on solar wind speed, solar rotation rate and colatitude. Measurements are available in the outer heliosphere at many tens of AU from Pioneer and Voyager. Recent Voyager observations extend the range out to 81 AU with the results shown in Fig. 4 that covers over two sunspot cycles with characteristic variations in  $B$ , high values near solar maximum and low values near solar minimum [11]. The overview shows the observed  $B$  and three versions of the Parker model as a function of distance beginning at launch in 1977. Measurements of  $V$  are not available at Voyager 1. The solid curve is derived by extrapolating the photospheric magnetic field to a potential field source surface to obtain the expansion factor and, therefore, the solar wind speed with which it is correlated [12]. Since the inaccuracies introduced by this procedure are difficult to assess,  $B$  is also calculated assuming a high speed of 800 km/sec (the upper dashed curve) and a low speed of 400 km/sec (the lower dashed curve). All three versions use the same spacecraft measurements at 1AU and extrapolate them outward to the location of Voyager.

## Voyager 1

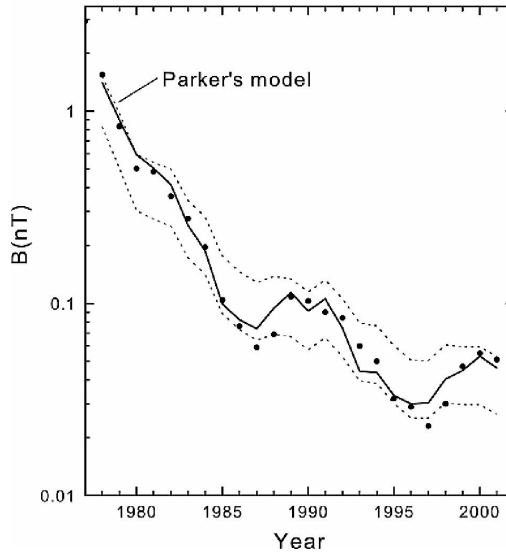


**FIGURE 4.** The field magnitude at Voyager 1 (closed dots) is shown along with three versions of the Parker model extrapolated outward from 1 AU. During the time interval shown, the spacecraft traveled from 1 to 81 AU. The heavy curve is the best estimate of  $B$  using an estimate of the variable solar wind speed while the dashed lines are for speeds of 800 and 400 km/sec. Although the measurements follow the Parker extrapolation fairly well in general, the observed field is significantly weaker near the two solar minima in 1986 and 1996. This being a log plot, these departures are actually a large fraction of the total field. (From [11])

Overall, the agreement between the Voyager observations and the Parker model is quite reasonable. Note, however, that the measured  $B$  is significantly smaller than the “best” estimate based on the Parker model,  $B_P$ , near the two solar minima in 1986 and 1996. When the semi-log plot is converted into a difference plot,  $(B_P - B)/B_P$ , the reduction near minimum is approximately 30% at 30 AU (and at 60 AU) or 1% per AU.

Relative differences of this magnitude have been reported in the past, principally in the Pioneer 10, 11 measurements and gave rise to a controversy over this so-called “flux deficit” [13]. The Pioneer data exhibit a decrease in  $B$  relative to  $B_P$  of about 1% per AU out to 30 AU with significantly larger decreases near solar minimum as seen here in the Voyager data. In part, the controversy appears to involve semantic differences. “Flux deficit” has been used with several different meanings. The term is used here to refer to an empirical difference between  $B$  and  $B_P$  (or  $B_T$  and  $B_{PT}$  since the field is essentially azimuthal at large distances) independent of specific models or interpretations. Some authors use the term to refer to a spreading of the field away from the solar equator that results in a reduction of magnetic flux at low latitudes. Several models have appeared that lead to this consequence among them enhanced pressure at low latitudes caused by the spiraling of the magnetic field or heating associated with fast-slow stream interactions (CIRs) [14, 15]. The discrepancy noted

above in rarefaction regions (dwells) where the field turns toward the radial direction is another potential contributor to the “flux deficit” that needs to be considered. The Voyager investigators dislike the term, “flux deficit”, and prefer to attribute the decreases near minimum to the formation of a “vortex street” in the solar wind [16]. From the point of view of this review, the important result is another discrepancy from the Parker model (at least during solar minimum and perhaps at other times as well).

## CONCLUDING REMARKS

An accurate description of the HMF in the outer heliosphere is important to many studies, for example, those involving galactic and anomalous cosmic rays. The Parker model describes the large-scale field to a fairly high degree of accuracy and undoubtedly may be used by theorists and others with some confidence. However, as has been shown above, evidence has accumulated of departures from the model in all the components and the field magnitude. In specific studies, caution is therefore necessary in deciding whether to continue using the Parker field or a modification of it such as one of the newer models now coming on line.

## ACKNOWLEDGMENTS

Results presented here represent one aspect of research carried out at the Jet Propulsion Laboratory, California Institute of Technology, under contract to the National Aeronautics and Space Administration.

## REFERENCES

1. E. N. Parker, *Interplanetary Dynamical Processes*, Interscience Publishers, New York, 1963, pp. 137–140.
2. E. J. Smith and A. Balogh, “Open Magnetic Flux: Variation with Latitude and Solar Cycle”, *Solar Wind Ten*, edited by M. Velli et al., AIP Conference Proceedings 679, Melville, New York, 2003, pp. 67–70.
3. E. J. Smith and A. Balogh, *Geophys. Res. Lett.* **22**, 3317–3320 (1995).
4. L. A. Fisk and N. A. Schwadron, *Astrophys. J.* **560**, 425–438 (2001).
5. E. J. Smith and A. Balogh, *Adv. Space Res.* **20**, 47–53 (1997).
6. M. Banaszkiewicz, W. I. Axford and J. F. McKenzie, *Astron. Astrophys.* **337**, 940–944 (1998).
7. N. Murphy, E. J. Smith and N. A. Schwadron, *Geophys. Res. Lett.* **29** (22), 23-1–23-4 (2002).
8. N. A. Schwadron, *Geophys. Res. Lett.* **29** (14), 8-1–8-4 (2002).
9. L. A. Fisk, *J. Geophys. Res.* **106**, 15,849–15,857 (2001).
10. D. Clack, R. J. Forsyth and M. W. Dunlop, *Geophys. Res. Lett.* **27**, 625–628 (2000).
11. L. F. Burlaga, N. F. Ness, Y.-M. Wang and N. R. Sheeley Jr., *J. Geophys. Res.* **107** (A11), SSH 20-1–SSH 20-11 (2002).
12. Y.-M. Wang and N. R. Sheeley Jr, *Astrophys. J.* **355**, 726–732 (1990).
13. D. Winterhalter, E. J. Smith, J. H. Wolfe and J. A. Slavin, *J. Geophys. Res.* **95**, 1–11 (1990).
14. S. T. Suess, B. T. Thomas and S. F. Nerney, *J. Geophys. Res.* **90**, 4378–4382 (1985).
15. V. J. Pizzo and B. E. Goldstein, *J. Geophys. Res.* **92**, 7241–7253 (1987).
16. L. F. Burlaga and J. D. Richardson, *J. Geophys. Res.* **105**, 10,501–10,507 (2000).